BIOSORPTION OF LOPERAMIDE BY LIGNOCELLULOSIC-Al_2O_3 HYBRID: OPTIMIZATION, KINETICS, ISOTHERMAL AND THERMODYNAMIC STUDIES

NENA VELINOV, SLOBODAN NAJDANOVIĆ, MILJANA RADOVIĆ VUČIĆ, JELENA MITROVIĆ, MILOŠ KOSTIĆ, DANIJELA BOJIĆ and ALEKSANDAR BOJIĆ

University of Niš, Faculty of Science and Mathematics, Department of Chemistry, Niš, Serbia
✉ *Corresponding author: N. Velinov, nena.velinov@yahoo.com*

Received April 12, 2018

Lignocellulosic biomass chemically modified with an inorganic oxide (Al_2O_3) was tested as a new sorbent for the removal of drug loperamide from water. Waste biomass generated from *Lagenaria vulgaris* plant was used as a lignocellulosic raw material. The effects of initial pH, temperature, sorbent dosage, initial loperamide concentration and hydrodynamic conditions on the sorption process were studied. The highest removal efficiency of loperamide was observed at neutral pH (5-8) and reached 99.5%, which is the greatest advantage of this hybrid. The maximal sorption capacity of the material was 48.74 mg/g. Sorption kinetics suggested that both surface reaction and diffusion were rate-limiting steps. The calculated thermodynamic parameters showed that the sorption process was feasible, spontaneous and endothermic. Also, the removal of loperamide from the river water was successfully carried out. The present study suggests that the obtained lignocellulosic-Al_2O_3 hybrid sorbent could be used effectively for the removal of loperamide from natural waters and wastewaters.

Keywords: lignocellulose, Al_2O_3, biosorption, loperamide, wastewater treatment

INTRODUCTION

The environmental effect of pharmaceuticals and personal care products (PPCPs) is largely speculative. PPCPs are substances used by individuals for personal health or cosmetic reasons and products used by agribusiness to boost the growth or health of livestock.[1] Medicines have an important role in the treatment and prevention of diseases in both humans and animals. However, it is because of the very nature of medicines that they may also have unintended effects on animals and microorganisms in the environment. PPCPs have been detected in water bodies throughout the world.[2] Drug pollution or pharmaceutical pollution is pollution of the environment with pharmaceutical drugs and their metabolites, which reach the aquatic environment (groundwater, rivers, lakes and oceans) through wastewater. Drug pollution is therefore mainly a form of water pollution and has been recognized as a potential environmental threat.[3] The European Union summarizes pharmaceutical residues with the potential of contamination of water and soil, together with other micropollutants, under "priority substances". Some pharmaceuticals can cast effects on bacteria and animals well below the concentrations that are usually used in safety and efficacy tests. In addition, breakdown products and the combination of different biologically active compounds may have unanticipated effects on the environment. Although it may be safe to assume that these substances do not substantially harm humans, researchers have only recently begun to investigate whether and how they affect a wide range of organisms in the environment and what this means for environmental health. There is a growing demand to find efficient, low-cost and easily available sorbents for the sorption of drugs. Among the emerging remediation technologies for drug impurity, biosorption of drugs using natural biomasses or agro-industrial wastes and by-products is known to be a feasible and efficient alternative considering numerous biosorbent sources, low operational costs, high removal efficiency and low secondary pollution risk.[4-6]

The ability of lignocellulosic biomass chemically modified with Al_2O_3 (LC-Al_2O_3) for biosorptive removal of the commonly used drug loperamide from water was studied in the present work. *Lagenaria vulgaris* shell was used as a starting lignocellulosic material for biosorbent synthesis. Biomass is mainly composed of three main components, namely cellulose, hemicelluloses and lignin.[7] *Lagenaria vulgaris* is a climbing plant with a long history of traditional medicinal uses in many countries. Since ancient times, this plant has been known for its curative properties and has been utilized for treatment of various diseases. Its fruit pulp and its extracts have been found to possess various pharmacological activities and potential uses in pharmaceutics.[8] After using the fruit pulp, the lignocellulosic plant shell is a waste material, which can be used for chemical modification with small amounts of Al_2O_3.

Loperamide, which is commercially available as loperamide hydrochloride (4-[4-(4-chlorophenyl)-4-hydroxypiperidin-1-yl]-N,N-dimethyl-2,2-diphenylbutanamide HCl), is an anti-diarrhoea drug for the fast and effective relief of diarrhoea associated with inflammatory bowel disease.[9,10] Loperamide has typically been deemed to have a relatively low risk of misuse and in 2012 there were no reports of loperamide abuse.[11,12]

In order to define the optimal conditions for the removal of loperamide from water by LC-Al_2O_3 hybrid, the following parameters were studied: initial pH, temperature, sorbent dosage, initial loperamide concentration and hydrodynamic conditions. We also applied common kinetics, isotherm and thermodynamic models that use various parameters, to determine the sorption mechanism, equilibrium and sorbent capacity.

EXPERIMENTAL

Material

Loperamide hydrochloride was purchased from Sigma-Aldrich. $Al(NO_3)_3x9H_2O$, trimethylamine, HNO_3, NaOH and $NaNO_3$ were of reagent grade (Merck, Germany). All the chemicals were used without further purification. All the solutions were prepared with deionized water (18 MΩ).

Preparation of biosorbent

Lignocellulosic biomass (*Lagenaria vulgaris* shell) was roughly crushed, washed with deionized water and ground by a laboratory mill. 10 g of biomass was acid treated with 300 mL 0.3 M HNO_3 in order to remove bio-accumulated metals. The suspension was stirred for 1 h on a magnetic stirrer and then the biomass was washed with deionized water until neutral pH. The biomass was then alkali treated with 150 mL 0.5 M NaOH for 60 min under heating. In this way, the hydrolysis of ester functional groups, swelling of cellulose and partial dissolution of lignin were performed, resulting in the formation of new carboxyl and hydroxyl groups on the surface of the biomass, which can be successfully chemically modified with Al_2O_3. After that, the biomass was washed with deionized water until neutral pH. Then, the biomass was dispersed in 100 cm^{-3} of solution containing 1 g of $Al(NO_3)_3{\times}9H_2O$ and the suspension was stirred for 0.5 h at 25.0±0.5 °C. After that, the solution was evaporated. The obtained material was treated for 2 h by trimethylamine vapour generated from liquid trimethylamine (commercial 40% aqueous solution), in order to provide alkaline medium for the formation of Al_2O_3 on the biomass surface. Then, the material was washed with deionized water until neutral pH and dried at 55±1 °C for 5 h. This material was denoted as LC-Al_2O_3.

Determination of pH_{pzc}

The point of zero charge was determined by the pH drift method with some modifications for LC-Al_2O_3 biosorbent.[13] As an inert electrolyte, 0.1 M $NaNO_3$ solution was used. The pH of a series of 100 mL electrolyte solutions was adjusted in the range between 2 and 10, using 0.1/0.01 M HNO_3 and 0.1/0.01 M KOH. These pH values were declared as initial (pH_i). Biosorbent samples (0.2 g) were added to 100 mL of test solutions in stoppered glass tubes and equilibrated for 24 h. The final pH (pH_f) was measured after 24 h and plotted against the initial pH (pH_i). The pH value at which the curve crosses the line $pH_i = pH_f$ was taken as pH_{pzc}.

Batch sorption experiments

Working model solutions were prepared by the appropriate dilution of the stock solutions (0.1000 g dm^{-3}). The pH of the solutions was adjusted with 0.1/0.01 mol dm^{-3} $NaOH/HNO_3$ solutions pH-metrically (Orion Star A214, Thermo Fisher Scientific, USA). In order to maintain a certain temperature, all the experiments were carried out in a water bath, by recirculating water from a Julabo F12-ED thermostatic bath (Refrigerated/Heating Circulator, Germany). In order to examine the hydrodynamic conditions and ultrasound power effect, experiments were conducted in an ultrasonic bath (Sonic, Serbia; total nominal power: 50 W) that operates at 40 kHz frequency. Aliquots of the solution were taken before the sorption started and after particular periods of time.

Loperamide concentration was determined using a Dionex Ultimate 3000 HPLC system (Thermo Scientific, USA). The system was controlled and data analyses were performed with Chromeleon 7 Data

Analysis software. The detector was set to 226 nm by isocratic elution with a flow rate of 1.5 cm^3 min^{-1}. The separation was carried out at 25 °C temperature, using a ZORBAX Eclipse XDB-C18 column (1.5 mm × 150 mm, 5 μm), with a mobile phase consisting of 0.1% sodium-octansulphonate, 0.05% triethylamine, 0.1% ammonium hydroxide (buffer) in water:acetonitrile (45:55 v/v). The mobile phase was adjusted to pH 3.2 with phosphoric acid. All the samples were filtered through a 0.45 μm millipore filter. The limit of detection (LOD) for this method is approximately 0.01 ppm.[14]

The amount of sorbed loperamide q_t (mg g^{-1}) and the removal efficiency of loperamide (*RE*) was determined by using Equations (1) and (2):

$$q_t = \frac{(c_0 - c_t)V}{m_s} \quad (1)$$

$$\mathrm{RE}(\%) = \frac{c_0 - c_t}{c_0} \cdot 100\% \quad (2)$$

where c_0 and c_t are the initial and final loperamide concentrations (mg dm^{-3}), V is the solution volume (dm^3) and m is the mass of the sorbent (g).

Relative deviation (RD) was calculated using Equation (3):

$$\mathrm{RD}(\%) = \frac{\left|q_{exp} - q_{cal}\right|}{q_{exp}} \cdot 100\% \quad (3)$$

Kinetic, isotherm and thermodynamic studies were performed by preparing solutions with the initial concentration of loperamide in the range from 5.0 to 100.0 mg dm^{-3}, and mixing the solutions at pH 7.0 with 2.0 g dm^{-3} of the sorbent, followed by agitating the mixture (150 rpm, at 25.0 °C) until equilibrium. All the parameters were evaluated with the non-linear regression method by means of OriginPro 2016 software (OriginLab Corporation, USA).

RESULTS AND DISCUSSION

Process optimization

Effect of pH

The pH of the solution plays an important role in the whole sorption process and has particular influence on the sorption capacity. It influences not only the surface charge of the sorbent, the degree of ionization of the material present in the solution and the dissociation of functional groups on the active sites of the sorbent, but also the chemistry of loperamide in the solution. The experiments were conducted varying the initial pH value from 2.0 up to 12.0, while the other parameters were kept constant (initial loperamide concentration: 20.0 mg dm^{-3}, sorbent dose: 2.0 g dm^{-3}, temperature: 25.0 ± 0.2 °C). The results showed that an increase in the solution pH from 1.0 to 5.0 led to an increase in the loperamide removal efficiency, while further increase in the solution pH up to 8 did not significantly influence the achieved high removal efficiency of loperamide. With further increase in the solution pH from 8.0 to 12.0, the removal efficiency decreased (Fig. 1). The highest removal efficiency of loperamide was observed at neutral pH (pH from 5.0 to 8.0) and reached 99.5%.

Depending on the surface charge of the biosorbent and the molecular charge of loperamide, sorption of the drug onto the surface may take place. Based on the pKa value (8.66), loperamide gets protonated in the acidic medium and deprotonated at higher pH. Consequently, the molecule has high positive charge density at a lower pH. The low sorption of loperamide in acidic solution is also due to the protonation of the sorbent surface groups. The pH at the point of zero charge (pH_{pzc}) of LC-Al_2O_3 has been found to be 5.85. At a pH below the pH_{pzc}, the sorbent surface is positively charged and anion sorption occurs. Otherwise, it would show negative charge, so that the extent of sorption of cations increased. Therefore, at a pH below 5.0 ($pH < pH_{pzc}$), electrostatic repulsion exists between the positively charged surface and the positively charged loperamide molecule. Also, lower sorption of loperamide at acidic pH is caused by the presence of excess H^+ ions competing with loperamide for the sorption sites. When the pH of the solution increases above 6.0 ($pH > pH_{pzc}$), the number of the negatively charged sites increases. Therefore, the sorption of loperamide increases at higher pH values and the process takes place more easily, confirming the presence of strong chemical interactions between the sorbate and the material. However, at a pH higher than 9.0 (pH > pKa), the sorption of loperamide decreases because of the repulsions between the negatively charged loperamide molecules and the negatively charged surface of the biosorbent. A similar trend for organic pollutants was reported by other authors.[15-19]

The fact that natural waters and typical wastewaters have neutral pH, in the application of the LC-Al_2O_3 hybrid for removing pollutants such as loperamide, there is no need for conditioning the pH value of water, so this is one of the greatest advantages of this material.

Effect of temperature

The temperature of the solution plays an important role in the sorption process. The temperature has two major effects on the sorption process. Increasing the temperature is known to

cause an increase the rate of diffusion of the sorbate molecules across the external boundary layer and in the internal pores of the sorbent, owing to the decrease in the viscosity of the solution. In addition, changing temperature will change the equilibrium capacity of the sorbent for a particular sorbate.[20,21]

The experiments were done at different temperatures: 10.0, 20.0, 35.0 and 50.0 °C, while other parameters were kept constant (initial pH 7.0, initial loperamide concentration 20.0 mg dm^{-3}, sorbent dose 2.0 g dm^{-3}). Results show that an increase in the solution temperature from 10.0 to 50.0 °C led to an increase of removal efficiency of loperamide (Fig. 2), indicating the process to be endothermic in nature. The removal efficiency of the process increased from 40.3% to 99.8%, with temperature from 10.0 to 50.0 °C. Such influence of temperature may be result of expected increasing of the diffusion of the large molecule as loperamide is, in water environment.[22]

Effect of sorbent dosage

The effect of sorbent dose on loperamide removal efficiency was investigated in the range from 0.5 to 8.0 g dm^{-3}, while the other parameters were kept constant (initial pH: 7.0, initial loperamide concentration: 20.0 mg dm^{-3}, temperature: 25.0 ± 0.2 °C). The results are presented in Figure 3. The removal efficiency of loperamide increased quickly from 26.6% to 99.5% by an increase in the sorbent dose from 0.5 g dm^{-3} to 2.0 g dm^{-3}, due to the increased active surface area of the biosorbent and the number of available binding sites for loperamide. Further increase of the sorbent dose to 4.0 g dm^{-3} slightly enhanced the removal efficiency to 99.7%. Removal efficiency remained almost unchanged at sorbent doses of 6.0 and 8.0 g dm^{-3}.

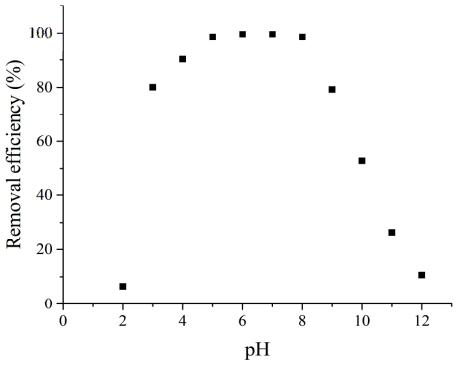

Figure 1: Effect of initial pH on loperamide sorption onto LC-Al_2O_3 hybrid (initial pH range: 2.0-11.0, initial loperamide concentration: 20.0 mg dm^{-3}, sorbent dose: 2.0 g dm^{-3}, temperature: 25.0 ± 0.2 ºC)

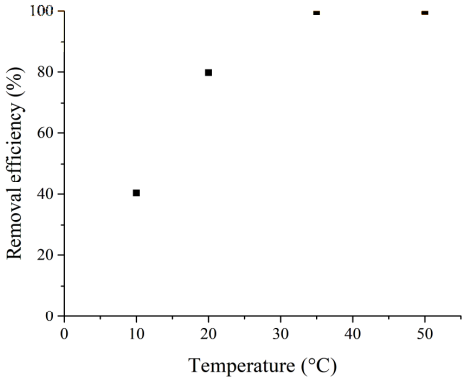

Figure 2: Effect of temperature on loperamide sorption onto LC-Al_2O_3 hybrid (initial pH 7.0, initial loperamide concentration: 20.0 mg dm^{-3}, sorbent dose: 2.0 g dm^{-3}, temperature range: 10.0-50.0 ºC)

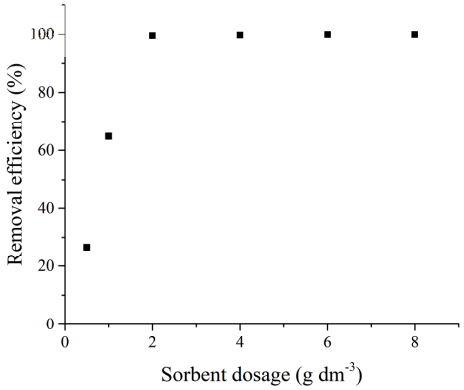

Figure 3: Effect of sorbent dose on loperamide sorption onto LC-Al_2O_3 hybrid (initial pH: 7.0, initial loperamide concentration: 20.0 mg dm^{-3}, sorbent dose: 0.5-8.0 g dm^{-3}, temperature: 25.0 ± 0.2 ºC)

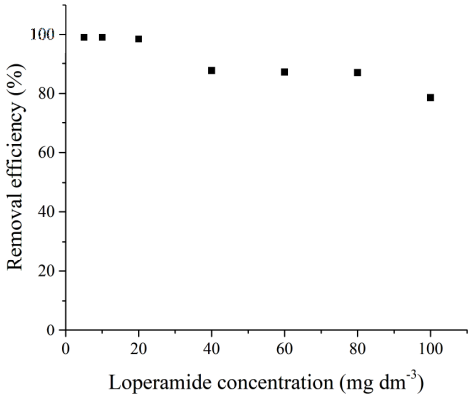

Figure 4: Effect of initial loperamide concentration on loperamide sorption onto LC-Al_2O_3 hybrid (initial pH: 7.0, initial loperamide concentration range: 5.0-100.0 mg dm^{-3}, sorbent dose: 2.0 g dm^{-3}, temperature: 25.0 ± 0.2 ºC

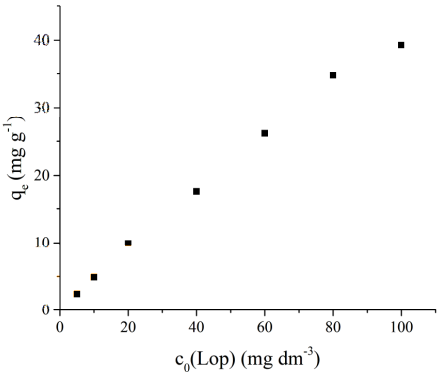

Figure 5: Effect of initial loperamide concentration on loperamide sorption onto LC-Al_2O_3 hybrid (initial pH: 7.0, initial loperamide concentration range: 5.0-100.0 mg dm^{-3}, sorbent dose: 2.0 g dm^{-3}, temperature: 25.0 ± 0.2 ºC

The negligible change in the removal efficiency at biosorbent dosages higher than 2.0 g dm^{-3} may be attributed to the presence of the excess of active centers for loperamide binding onto the biosorbent surface, with regard to the initial concentration of loperamide. Therefore, the value of 2.0 g dm^{-3} was considered as the optimal biosorbent dose of LC-Al_2O_3 for loperamide removal, and it was used in all further experiments. A similar effect was reported by other authors.[23-25]

Effect of initial loperamide concentration

The effect of initial loperamide concentration on the removal efficiency was investigated in the range from 5.0 to 100.0 mg dm^{-3}, while the other parameters were kept constant (initial pH: 7.0, sorbent dose: 2.0 g dm^{-3}, temperature: 25.0 ± 0.2 °C) (Fig. 4). With an increase in initial loperamide concentration, the removal efficiency decreased. For the initial loperamide concentration of 5.0, 10.0 and 20.0 mg dm^{-3}, the removal efficiency was very high, of 99.9, 99.8 and 99.5%, respectively. With further increase in loperamide concentration from 40.0 to 80.0 mg dm^{-3}, the removal efficiency slowly decreased. For the initial loperamide concentration of 100.0 mg dm^{-3}, the removal efficiency was minimal and amounted to 78.6%.

In the case of the lower concentrations investigated (5.0, 10.0 and 20.0 mg dm^{-3}), the ratio of the initial number of loperamide molecules to the available sorption sites is low and the biosorption becomes independent of initial concentration, which enabled the 99% loperamide uptake. At the higher concentrations investigated (up to 100.0 mg dm^{-3}), a certain amount of loperamide is left unsorbed in the solution because of the saturation of the limited available binding sites in the biomass sorbent. Therefore, the removal of loperamide depends on its initial concentration, as in the case of plenty other similar pollutants.[17,23,25,26]

However, the biosorption capacity of loperamide increases with increasing initial loperamide concentration (Fig. 5), and reaches 45.28 mg g^{-1} at 100.0 mg dm^{-3} initial concentration of loperamide and 2.0 g dm^{-3} dose of biosorbent. This can be attributed to the fact that the higher loperamide concentrations increase the overall mass transfer driving force and thus the loperamide is absorbed by the biosorbent.[27]

Effect of hydrodynamic conditions

The effect of hydrodynamic conditions was investigated at different ultrasound power, from 0 to 50 W. Ultrasound, through its mechanical waves, has been used as a means for enhancing the sorption process. Ultrasonic waves strongly enhance mass transfer between two phases by reducing the thickness of liquid films on the solid phase and thus the diffusion is enhanced.[28] The effect of hydrodynamic conditions on loperamide sorption was investigated at ultrasonic irradiation acoustic power of 0, 25 and 50 W, while the other parameters were kept constant (initial pH: 7.0, initial loperamide concentration: 20.0 mg dm^{-3}, sorbent dose: 2.0 g dm^{-3}, temperature: 25.0 ± 0.2 °C) (Fig. 6). It is clear from the results that the presence of ultrasound does not change the

removal efficiency of loperamide, but it speeds up the sorption process a lot. The removal efficiency in all the three cases of different ultrasound power is 99.5%. In the absence of ultrasound, equilibrium is attained after a period of time of 120 min. Meanwhile, in the presence of ultrasound, at power levels of 25 and 50 W, the equilibrium is attained considerably faster, after 40 and 20 min, respectively. The stronger the acoustic power is, the greater is the intensity of the ultrasonic field, which leads to an improvement of microstreaming, microturbulence, shock waves and microjets and to an enhancement of mass transfer in the system, speeding up the process of loperamide sorption.[29]

Sorption kinetics

The kinetics of loperamide sorption onto the LC-Al_2O_3 hybrid can be described by the pseudo-first order model, pseudo-second order model, intraparticle diffusion kinetic model and Chrastil diffusion model. The equations and parameters of all the above-mentioned kinetic models, along with their corresponding r^2 values, are presented in Table 1.

Reaction kinetics

The pseudo-first order kinetic model describes the rate of sorption, which is proportional to the number of unoccupied binding sites of the sorbent.[30] The pseudo-second order kinetic model is based on equilibrium sorption, which depends on the amount of solute sorbed on the surface of sorbent and the amount sorbed at equilibrium.[31] In the non-linear equations of the pseudo-first order and pseudo-second order kinetic models (Table 1), k_1 (min^{-1}) is the first-order rate constant, k_2 (g mg^{-1} min^{-1}) is the second-order rate constant, q_t and q_e (mg g^{-1}) are the amounts of loperamide sorbed at time t and at equilibrium, respectively. The values for the pseudo-first and pseudo-second order constants, k_1 and k_2, the amount of the loperamide sorbed at equilibrium, q_e, the determination coefficients and relative deviation for both models, for the sorption of different initial loperamide concentrations, are listed in Table 1.

As can be seen from the data presented in Table 1, the determination coefficients for the pseudo-first order kinetics obtained by non-linear analysis are relatively high for all the studied initial loperamide concentrations. Likewise, the determined values of q_e calculated from Lagergren's equation showed similarity with the experimental values, which indicated that the pseudo-first order kinetic model can predict the sorption of loperamide onto the LC-Al_2O_3 hybrid. The calculated q_e values obtained by the pseudo-second order kinetic model were very close to the experimental q_e values, suggesting that the kinetics of biosorption of loperamide by the LC-Al_2O_3 hybrid follows very well the pseudo-second order model. With increasing initial loperamide concentration from 5.0 up to 100.0 mg g^{-1}, the pseudo-second order rate constant, k_2, decreased from 0.332 to 0.053 g mg^{-1} min. At a lower initial loperamide concentration, almost all the binding sites were free, which resulted in high pseudo-second rate constant, while at a higher loperamide concentration, saturation of the sorption sites occurred and the value of k_2 decreased.

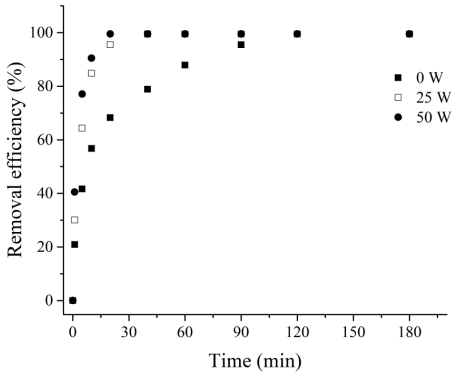

Figure 6: Effect of hydrodynamic conditions on loperamide sorption onto LC-Al_2O_3 hybrid (initial pH: 7.0, initial loperamide concentration: 20.0 mg dm^{-3}, sorbent dose: 2.0 g dm^{-3}, temperature: 25.0 ± 0.2 ºC)

Table 1
Kinetic parameters for loperamide sorption onto LC-Al_2O_3 hybrid

c (mg dm^{-3})	5	10	20	40	60	80	100
q_e, exp (mg g^{-1})	2.36	4.73	9.43	18.51	27.23	34.76	39.28
Pseudo-first-order model, $q_t = q_e(1-e^{k_1 t})$							
q_e, cal (mg g^{-1})	2.30	4.60	9.18	17.73	26.10	33.05	36.42
k_1 (min^{-1})	0.180	0.145	0.203	0.089	0.050	0.037	0.034
r^2	0.975	0.974	0.963	0.952	0.952	0.933	0.916
RD (%)	2.54	2.75	2.65	4.21	4.15	4.92	7.28
Pseudo-second-order model, $q_t = \frac{q_e^2 k_2 t}{1 + k_2 q_e t}$							
q_e, cal (mg g^{-1})	2.36	4.74	9.42	18.54	27.69	35.30	39.07
k_2 (g mg^{-1} min^{-1})	0.332	0.254	0.386	0.143	0.078	0.059	0.053
r^2	0.993	0.992	0.992	0.989	0.988	0.978	0.971
RD (%)	0	0.21	0.11	0.16	0.68	1.52	1.53
Intraparticle diffusion model, $q_t = k_d t^{1/2} + C$							
k_{i1} (mg g^{-1} min$^{-1/2}$)	0.580	1.055	2.301	2.622	2.778	3.178	3.390
C_1 (mg g^{-1})	0.04	0.09	0.42	0.86	2.07	2.65	3.02
r^2	0.979	0.990	0.972	0.971	0.957	0.956	0.945
k_{i2} (mg g^{-1} min$^{-1/2}$)	0.114	0.121	0.240	0.565	0.623	0.731	0.821
C_2 (mg g^{-1})	1.53	3.53	7.22	10.94	19.17	21.72	22.94
r^2	0.962	0.942	0.891	0.929	0.804	0.968	0.942
k_{i3} (mg g^{-1} min$^{-1/2}$)	0.006	0.014	0.018	0.058	0.061	0.088	0.216
C_3 (mg g^{-1})	2.22	4.42	9.04	17.17	26.19	34.09	34.10
r^2	0.904	0.814	0.814	0.955	0.953	0.766	0.921
Chrastil diffusion model, $q_t = q_e\left(1-e^{-k_C A_0 t}\right)^n$							
q_e, cal (mg g^{-1})	2.32	4.65	9.31	18.27	27.06	34.78	39.26
k_C	0.041	0.031	0.034	0.011	0.008	0.005	0.003
n	0.471	0.462	0.379	0.365	0.406	0.373	0.341
r^2	0.995	0.996	0.997	0.998	0.999	0.999	0.999

Equilibrium sorption capacity, q_e, calculated by non-linear regression, increased almost linearly from 2.36 mg g^{-1} up to 27.69 mg g^{-1} with an increase in initial loperamide concentration from 5.0 mg dm^{-3} to 60.0 mg dm^{-3}, and slightly to 39.07 mg g^{-1} with a further increase in initial loperamide concentration up to 100.0 mg g^{-1}. This can also be related to the saturation of binding sites on the sorbent surface.

The obtained determination coefficients for the pseudo-second order model (0.993-0.971) are higher than the determination coefficients for the pseudo-first order model (0.975-0.916) for all the tested concentrations (5.0-100.0 mg dm^{-3}). The obtained relative deviation for the pseudo-second order model (0-1.53%) is lower than the deviation for the pseudo-first order model (2.54-7.28%) for all the tested concentrations (5.0-100.0 mg dm^{-3}).

The experimental data showed that the pseudo-second order model fitted better the experimental data than pseudo-first order model, due to a higher determination coefficient, better match of the experimental to the calculated q_e values and lower value of relative deviation obtained in all the cases. The obtained results indicate that the pseudo-second order model can be successfully used for the study of loperamide sorption by the LC-Al_2O_3 hybrid and suggest that the mechanism may be presented as a surface reaction occurring *via* sharing or exchange of electrons between the sorbent and the sorbate.[32,33]

Diffusion kinetics

Intraparticle diffusion model. The sorbate transport from the solution phase to the surface of the sorbent particles occurs in several steps: bulk diffusion, external (film) diffusion, intraparticle diffusion and finally, sorption of the sorbate onto the sorbent surface. The overall sorption process may be controlled by either one or more steps. The possibility of intraparticle diffusion was explored by using the intraparticle diffusion kinetics model.[34] In the equation of this model (Table 1), C is the intercept and k_{id} is the intraparticle diffusion rate constant (mg g^{-1} min$^{-1/2}$) determined from a plot of q_t *versus* $t^{1/2}$. If this

plot satisfies the linear relationship with the experimental data, then intraparticle diffusion is a rate controlling step; if the data exhibit multi-linear plots, then some degree of boundary layer control might be present and two or more steps influence the sorption process. The values of C provide an idea about the thickness of the boundary layer: the larger the intercept, the greater the boundary layer effect.[35]

The regression of q_t *versus* $t^{1/2}$ for the sorption of loperamide onto the LC-Al_2O_3 hybrid is not linear, suggesting that the intraparticle diffusion is not the only rate-controlling step. The intraparticle diffusion model for all the studied initial loperamide concentrations showed multi-linearity and three sorption stages. Similar results were reported in other studies, where the authors fitted kinetic data by three linear lines with a different slope.[36,37]

The first, sharper portion of the plot can be attributed to the diffusion of loperamide through the solution of the external sorbent surface, or the boundary layer diffusion of solute molecules. It is a rate limiting process at the beginning of the sorption. The second portion described the gradual sorption stage, where intraparticle diffusion was rate limiting. The third portion was attributed to the final equilibrium stage for which the intraparticle diffusion started to slow down because of the extremely low loperamide concentration left in the solution. It could be deduced that there were three processes that controlled the rate of molecule sorption, but only one was rate limiting in any particular time range. The slope of the linear portion indicated the rate of the sorption. The lower slope corresponded to a slower sorption process.

With an increase of initial loperamide concentration, the values of the rate constants for intraparticle diffusion k_{id1} and k_{id2} shown in Table 2 also increased. The increase in the value of the constants for intraparticle diffusion k_{id1} and k_{id2} indicates a greater driving force with increasing initial loperamide concentration (bulk liquid concentration raises the driving force of loperamide to transfer from the bulk solution onto and into the solid particle). Based on the values of k_{id1} and k_{id2}, it can be concluded that film diffusion is more efficient than intraparticle diffusion.

In addition, the C_1 and C_2 (measure of thickness of the boundary layer) values varied like the k_{id} values with initial loperamide concentration (Table 1), indicating film diffusion as the rate limiting step. A larger C value corresponds to a greater boundary layer diffusion effect.

The intraparticle diffusion rate constant, k_{i3}, was determined from the slope of the third portion of the plot, while the increment represents constant C. The calculated intraparticle diffusion rate constants (Table 1) increased from 0.006 to 0.216 mg g^{-1} $min^{-1/2}$ with increasing initial loperamide concentration from 5.0 to 100.0 mg dm^{-3}, which can be related to faster diffusion, thus also biosorption, because a higher initial loperamide concentration produces a stronger driving force for diffusion. In addition, constant C_3, which is taken to be proportional to the extent of boundary layer thickness, increased from 2.22 to 34.10 with increasing initial loperamide concentration, indicating decreases in the rate of the external mass transfer and hence increases in the rate of internal mass transfer.

Chrastil's diffusion model. Chrastil's diffusion model describes sorption kinetics in diffusion controlled systems.[37] In the mathematical equation of this model (Table 1), k_C is a rate constant (dm^3 g^{-1} min^{-1}), which depends on the diffusion coefficients and the sorption capacity of the biosorbent, A_0 is the dose of biosorbent (g dm^{-3}) and n is a heterogeneous structural diffusion resistance constant, which can range from 0 to 1. Constant n is independent of the sorbate concentration, sorbent concentration A_0, q_e and temperature.[35,38] In systems with small diffusion resistance, parameter n approximates 1, while the more significant resistance parameter n assumes small values (<0.5).

The parameters of the model: q_e, k_C and n, for the sorption of loperamide at initial concentration from 5.0 up to 100.0 mg dm^{-3} were determined by non-linear regression analysis of the experimental data and given in Table 1.

The obtained high determination coefficients, larger than 0.99 (Table 1), indicate a very good fit of the experimental kinetic data with Chrastil's model, for all the tested concentrations (5.0-100.0 mg dm^{-3}). The applicability of this diffusion model also confirms similar values of the calculated q_e with the experimentally determined q_e (Table 1). The results obtained for the diffusion resistance coefficient show that n values decrease from 0.471 to 0.341 (Table 1) for initial loperamide concentration from 5.0 up to 100.0 mg dm^{-3}. Low values of constants n mean that the sorption rate is strongly limited by the diffusion resistance.[39]

Adsorption isotherm

In this work, different biosorption equilibrium models of two (Langmuir, Freundlich, Temkin) and three (Redlich-Peterson, Sips, Toth, Khan, Hill and Brouers-Sotolongo) parameters were evaluated to fit the experimental LC-Al_2O_3 biosorption of loperamide. The isotherm equations and parameters, deduced from the experimental data by non-linear regression of the plot q_e *versus* c_e for all the above-mentioned models, along with their corresponding r^2 values, are presented in Table 2.

Table 2
Isotherm parameters for loperamide sorption onto LC-Al_2O_3 hybrid

Adsorption isotherm	Parameter	Values
Langmuir, $q_e = \frac{q_m K_L c_e}{1+K_L c_e}$, $\theta = \frac{K_L c_0}{1+K_L c_0}$, $R_L = \frac{1}{(1+K_L c_0)}$	K_L (dm^3 mg^{-1})	0.216
	q_m (mg g^{-1})	48.74
	r^2	0.997
Freundlich, $q_e = K_F c_e^{1/n}$	K_F, (mg g^{-1})$^{1/n}$	10.56
	n	2.182
	r^2	0.932
Tempkin, $q_e = \frac{RT}{b_T}\ln(K_T C_e) = B\ln(K_T C_e)$	K_T	3.293
	B (J mol^{-1} K^{-1})	9.189
	R^2	0.972
Redlich–Peterson, $q_e = \frac{K_{RP} c_e}{1+\alpha_{RP} c_e^{\beta}}$	K_R	8.898
	α_R	0.114
	β	1.146
	r^2	0.999
Sips, $q_e = \frac{q_m K_S c_e^{1/n}}{1+K_S c_e^{1/n}}$	q_m (mg g-1)	45.632
	K_S (dm^3 mg^{-1})	0.252
	n	1.118
	r^2	0.999
Toth, $q_e = \frac{K_T c_e}{(\alpha + c_e)^{1/t}}$	K_T	168.83
	α_T	8.945
	t	0.754
	r^2	0.999
Khan, $q_e = \frac{q_m b_K c_e}{(1+b_K c_e)^{\alpha}}$	q_m (mg g^{-1})	82.83
	b_K	0.111
	a_K	1.324
	r^2	0.999
Hill, $q_e = \frac{q_H c_e^{n_H}}{K_D + c_e^{n_H}}$	q_m (mg g^{-1})	45.63
	n_H	1.118
	K_D	4.655
	r^2	0.998
Brouers–Sotolongo, $q_e = q_m(1-\exp(-Kc_e^{\alpha}))$	q_m (mg g^{-1})	39.93
	K	0.226
	a	0.940
	r^2	0.999

Two-parameter isotherm models

The Langmuir model assumes that the uptake of adsorbate occurs on an energetically homogeneous surface by monolayer adsorption without any interaction between adsorbed species.[40,41] In the non-linear equation of the Langmuir isotherm model (Table 2), q_e is the amount of sorbate sorbed at equilibrium (mg g^{-1}), c_e is the equilibrium concentration of the sorbate in solution (mg dm^{-3}), q_m is the maximum sorption capacity (mg g^{-1}), and K_L is a Langmuir constant related to the energy of sorption, which reflects quantitatively the affinity between the sorbate and the sorbent. Maximum sorbate uptake q_m and Langmuir constant K_L can be deduced from the experimental data by a non-linear regression of the plot q_e *versus* c_e and they are presented in Table 3.

The favorability of the sorbate sorption process onto the sorbent was evaluated using a dimensionless parameter (R_L) derived from the Langmuir expression.[41] The R_L parameter is a

coefficient related to the energy of adsorption and increases with increasing strength of the adsorption bond. The adsorption process can be defined as irreversible ($R_L = 0$), favorable ($0 < R_L < 1$), linear ($R_L = 1$) or unfavorable ($R_L > 1$) in terms of R_L.

To account for the sorption behavior of the sorbate onto the biosorbent, the Langmuir type equation related to surface coverage (θ) is used.

The highest correlation factors ($r^2 > 0.99$) of the Langmuir model for loperamide indicates that the Langmuir model gives the best fit to the experimental data and so the sorption nature of drug loperamide on the sorbent surface is more compatible with the Langmuir assumptions, implying that the sorption of the investigated pollutant onto the sorbent is a mono-layer process and after saturation of this layer no further sorption took place.

The Langmuir isotherm shows that the amount of loperamide sorption increases as the concentration increases up to a saturation point. The maximum biosorbent capacity determined from the Langmuir isotherm model for loperamide was 48.74 mg g^{-1} (Table 2), which is consistent with the experimental value (45.28 mg g^{-1}).

The Langmuir model predicted an equilibrium constant (K_L) of 0.216 dm^3 mg^{-1} (Table 3), and this was used to calculate the Hall separation factor (R_L) and the surface coverage (θ) (Table 3). The first is indicative of the biosorption isotherm shape that predicts whether a biosorption isotherm is "favorable" or "unfavorable", while the latter indicates the fraction of the biosorption sites occupied by loperamide at equilibrium.

The separation factor decreased from 0.48 to 0.04 as the initial loperamide concentration increased from 5.0 to 100.0 mg dm^{-3}, which indicates that the biosorption of loperamide onto LC-Al_2O_3 increased as the initial loperamide concentration rose. Furthermore, the R_L values are between 0 and 1, indicating that the loperamide biosorption by the LC-Al_2O_3 hybrid is favorable at all the assayed loperamide concentrations, confirming the suitability of the biosorbent for the sorbate.[42] The surface coverage (θ) values approached unity (from 0.52 to 0.96) with increasing initial loperamide concentration, which indicates that the LC-Al_2O_3 surface was almost completely covered by a monomolecular layer of loperamide molecules at high loperamide concentrations. It is also apparent that the surface coverage ceased to vary significantly at higher loperamide concentrations and that the reaction rate became almost independent of the loperamide concentration. The θ values indicated effective biosorption of loperamide from aqueous solutions by the LC-Al_2O_3 hybrid at all the initial loperamide concentrations assayed.

The Freundlich empirical adsorption isotherm equation is based on adsorption onto a heterogeneous surface. It is assumed that the stronger binding sites are occupied first and that the binding strength decreases with the increasing degree of site occupation.[43] In the non-linear equation of the Freundlich isotherm model (Table 2), q_e is the amount of sorbate sorbed at equilibrium (mg g^{-1}), c_e is the equilibrium concentration of the sorbate in the solution (mg dm^{-3}), K_f is the Freundlich constant, related to the sorption capacity and $1/n$ is the Freundlich exponent, related to the intensity of sorption, which varies with the heterogeneity of the sorbent surface. When $1/n = 1$, the free energy for all the sorbate concentrations is constant; when $1/n < 1$, the added sorbate has weaker and weaker free energies, finally when $1/n > 1$, more sorbate present in the sorbent enhances the free energies of further sorption. The parameter n is related to the sorption energy distribution: when $n = 1$ then the partition between the two phases is independent of the concentration; when n lies between one and ten, this indicates a favorable sorption process.

Differences between the monolayer (chemisorption) and multilayer (physisorption) process can be detected by applying the Freundlich model. From the data in Table 2, the value of $1/n = 0.46$, while n = 2.18, indicating that the sorption of loperamide onto LC-Al_2O_3 hybrid is favourable and the r^2 value is 0.933, as noted in previous sorption works.[44-47] These values also suggest the formation of an almost homogeneous surface.

The Temkin isotherm assumes that the heat of sorption of all the molecules in a layer decreases linearly due to sorbent–sorbate interactions and that sorption is characterized by uniform distribution of binding energies, up to some maximum binding energy.[48] In the equation of the Temkin isotherm model (Table 2), constant $B = RT/b_T$ is related to the heat of sorption, R is the universal gas constant (J mol^{-1} K^{-1}), T is the absolute temperature (K), b_T is the variation of sorption energy (J mol^{-1}) and K_T is the equilibrium binding constant (dm^3 mg^{-1}) corresponding to the maximum binding energy.

The high value of r^2 (0.973) showed that, in addition to the Langmuir isotherm, the sorption process can also be represented by the Temkin isotherm model. The relatively high value of parameter *B* (9.189) indicates that there is a significant ionic interaction between loperamide and LC-Al_2O_3, suggesting the predominance of chemical sorption.

Three-parameter isotherm models

The Redlich–Peterson isotherm is an empirical isotherm incorporating three parameters.[49] It combines elements from both the Langmuir and Freundlich equations, while the mechanism of adsorption is a hybrid and does not follow ideal mono-layer adsorption. In the Redlich–Peterson isotherm equation (Table 2), K_{RP} is the Redlich–Peterson isotherm constant ($dm^3\ g^{-1}$), α_{RP} is also a constant having the unit of mg^{-1} and β is an exponent that lies between 0 and 1. If $\beta = 1$, then the Langmuir will be the preferable isotherm, while if $\beta = 0$, the Freundlich isotherm will be preferred.

The Sips isotherm is a combined form of the Langmuir and Freundlich expressions used for predicting the heterogeneous adsorption systems and circumventing the limitation of the rising sorbate concentration associated with the Freundlich isotherm model.[50] At low adsorbate concentrations, it reduces to the Freundlich isotherm; while at high concentrations, it predicts a mono-layer adsorption capacity characteristic of the Langmuir isotherm. In the Sips isotherm equation (Table 2), q_m is the Sips maximum adsorption capacity ($mg\ g^{-1}$), K_S is the Sips equilibrium constant ($dm^3\ mg^{-1}$), and $1/n$ is the Sips model exponent. The heterogeneity factor of n, close to or even equal to 1, shows a biosorbent with comparatively homogenous binding sites, while n close to 0 indicates a heterogeneous biosorbent. In other words, if $n = 1$, then the Langmuir model will be preferable isotherm, while if $n = 0$, the Freundlich isotherm will be preferred.

The Toth isotherm is derived from the potential theory, and it is applicable for heterogeneous adsorption.[51] This model assumes quasi-Gaussian energy distribution, where most sites have adsorption energies lower than the peak or maximum adsorption energy. In the Toth isotherm equation (Table 2), K_T is the Toth model constant and *t* is the Toth model exponent. For $t = 1$, this isotherm reduces to the Langmuir adsorption isotherm equation; therefore the parameter *t* is said to characterize the system heterogeneity. If it deviates further away from unity, the system is said to be more heterogeneous.

In the simplified form of the Khan model (Table 2), b_K is the Khan model constant and a_K is the Khan model exponent.[52]

Hill's equation was postulated to explain the binding of various species onto homogeneous substrates.[53] The model assumes that adsorption is a cooperative phenomenon, with the ligand binding ability at one site on the macromolecule, it may influence different binding sites on the same macromolecule. In this isotherm equation (Table 3), K_D, n_H and q_H are constants.

Brouers–Sotolongo proposed an isotherm for heterogeneous surfaces containing micro-cores.[54] In this isotherm equation (Table 2), c_e, *K* and α are equilibrium concentration ($mg\ dm^{-3}$), maximum adsorption capacity of the substrate ($mg\ g^{-1}$) and Brouers–Sotolongo isotherm constant, respectively. The parameter α is related to the degree of surface heterogeneity.[55]

The fits of the experimental data to the Redlich–Peterson, Sips, Toth, Khan, Hill and Brouers–Sotolongo isotherms are shown in Table 2 and the results indicate that all the three-parameter models have very a high r^2 value (0.999 in all the cases). The Brouers–Sotolongo isotherm shows the q_m value (39.93 $mg\ g^{-1}$) lower than that of the Langmuir isotherm value. On the other hand, the Sips and Hill isotherms show equal q_m value (45.63 $mg\ g^{-1}$), which is consistent with the experimental value (45.28 $mg\ g^{-1}$).

It is clear from the results that the Langmuir model and all the three-parameter models tested showed a good fit to the experimental equilibrium data. Furthermore, according to the r^2 values, neither the Langmuir model nor the three-parameter models showed any added advantage (Table 2). However, the value of the exponent of the Redlich–Peterson ($B_{RP} = 1.14693$), Sips ($n_s = 1.11859$) and Toth ($n_{To} = 0.75476$) models were close to 1, for which value these isotherm models are effectively reduced to the Langmuir model.[56] In addition, from a practical point of view, the Langmuir model is simpler than the three-parameter models and can consequently be applied and interpreted easier and is likely to be more helpful. Thus, the experimental equilibrium

data for the biosorption of loperamide by the LC-Al_2O_3 hybrid should preferably be fitted to the Langmuir model, which has practical importance for engineering design and scale-up.

Thermodynamics of biosorption

Thermodynamic parameters, including the change in free energy (ΔG^o), enthalpy (ΔH^o) and entropy (ΔS^o), were used to describe the thermodynamic behavior of the biosorption of loperamide on the LC-Al_2O_3 hybrid. Thermodynamic parameters were calculated from Equations (4) and (5):

$$\ln K_D = \frac{\Delta S^o}{R} - \frac{\Delta H^o}{RT} \quad (4)$$

$$\Delta G^o = \Delta H^o - T\Delta S^o \quad (5)$$

where R is the universal gas constant (8.314 J mol^{-1} K^{-1}), T is temperature (K) and K_D is the distribution coefficient calculated as the ratio of loperamide concentration sorbed at equilibrium and loperamide concentration remaining in the solution at equilibrium.[57]

The experiments were carried out at 283, 293, 308 and 323 K. The enthalpy and the entropy change of biosorption were estimated from the slope and intercept of the linear regression of $\ln K_L$ *vs*. 1000/T plot (Fig. 7). These thermodynamic parameters are given in Table 3. The free energy change was calculated to be –22.32, –24.41, –27.09 and –30.17 kJ mol^{-1} for the biosorption of loperamide at 283, 293, 308 and 323 K, respectively. The negative values of ΔG^o indicate the feasibility of the biosorption process and its spontaneous nature. The decrease in ΔG^o values with the increase in temperature shows a slight increase in the feasibility of biosorption at higher temperatures. The positive ΔH^o (32.56 kJ mol^{-1}) value implies the endothermic character of the process of biosorption within the analyzed range of temperatures (10.0-50.0 °C). The enthalpy value within 2.1-20.9 kJ mol^{-1} points to physical sorption, whereas the value from 80 to 200 kJ mol^{-1} indicates chemisorption. So, the values of ΔH^o in Table 3 indicate that loperamide sorption on the LC-Al_2O_3 hybrid should be attributed to a physico-chemical sorption process rather than to a pure physical or chemical sorption process.[58,59] The positive ΔS^o value (Table 3) suggests an increase in the randomness at the solid/solution interface during the biosorption of loperamide onto the LC-Al_2O_3 hybrid, and corroborates the previously proposed spontaneity of the biosorption process.[60,61]

Comparative analysis of drug sorption capacity of various biosorbents

For the purpose of comparison, Table 4 presents the maximum sorption capacity of the LC-Al_2O_3 hybrid biosorbent for loperamide removal along with the data for different drugs removed by other biosorbents reported in the literature. The sorption rate was noticed to be different according to biomass source, modification and type of pollutant.

It is clear from Table 4 that the sorption capacities for pharmaceutical compounds of costly carbonaceous biomass materials are higher than that of the LC-Al_2O_3 hybrid biosorbent. On the other hand, it is noticeable that the LC-Al_2O_3 hybrid biosorbent displayed an interesting potential among the rest of the biosorbents, especially considering its cost-effectiveness, ease of sorbent preparation, biocompatibility and environmental friendliness.

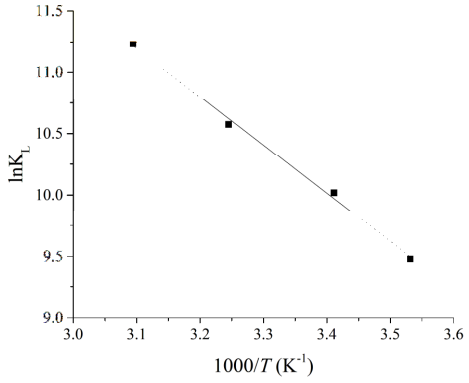

Figure 7: Thermodynamic parameters for loperamide sorption onto LC-Al_2O_3 hybrid

Table 3
Thermodynamic parameters for loperamide sorption onto LC-Al_2O_3 hybrid

$\Delta S°$ (J mol^{-1} K^{-1})	$\Delta H°$ (kJ mol^{-1})	$\Delta G°$ (kJ mol^{-1})			
		283 K	293 K	308 K	323 K
193.98	32.56	–22.32	–24.41	–27.09	–30.17

Table 4
Comparison of drug sorption capacity onto various biosorbents

Biosorbent	Pharmaceutical	q_m (mg g^{-1})	Source
Carbonaceous saw dust	Sulfamethoxazole	295.06	[62]
Carbonaceous saw dust	Tetracycline	270.53	[62]
Carbonaceous saw dust	Bisphenol A	263.75	[62]
Eucalyptus sawdust biochar	Dimetridazole	200.0	[63]
Eucalyptus sawdust biochar	Methronidazole	167.5	[63]
Aerobic granular sludge	Oxytetracycline	91.74	[64]
Rice straw	Clofibric acid	126.3	[65]
Parthenium hysterophorus biochar	Ibuprofen	90.46	[66]
Mung bean husk biochar	Ibuprofen	59.76	[67]
Lignocellulosic-Al_2O_3 hybrid	Loperamide	48.74	This study
Rice straw	Carbamazepine	40.0	[65]
Living microalga *Chlorella vulgaris*	Flutamide	26.8	[68]
Natural cellulose	Ranitidine	23.41	[69]
Dead microalga *Chlorella vulgaris*	Flutamide	12.5	[68]
Activated sludge	Ciprofloxacin	3.39	[70]
Activated sludge	Norfloxacin	3.24	[70]
Activated sludge	Ofloxacin	1.50	[70]
Aerobic granular sludge	Ciprofloxacin	2.94	[70]
Aerobic granular sludge	Norfloxacin	2.73	[70]
Aerobic granular sludge	Ofloxacin	1.18	[70]

River water treatment

To test the efficiency of the LC-Al_2O_3 hybrid for the removal of loperamide from contaminated water, river water was used for the sorption solution. By previous optimization of the purification process, the optimal dose of the LC-Al_2O_3 hybrid needed for the removal of loperamide was 2 g for 1.0 dm^{-3} of river water contaminated with loperamide, with a native initial pH of 6.5 and temperature of 25.0 °C. The advantage of the LC-Al_2O_3 hybrid is precisely the lack of need to adjust the pH value of polluted water for the removal of this kind of pollutants. The concentration of loperamide in the sample was 20 mg dm^{-3}. The results have shown that the removal of loperamide from contaminated river water was very effective and the removal efficiency was identical to those achieved in synthetic model solutions (99.5%). The high removal efficiency of loperamide from river water by the LC-Al_2O_3 hybrid indicates the great application potential of this material for this kind of organic pollutants.

CONCLUSION

A new hybrid material, based on lignocellulosic biomass chemically modified with Al_2O_3, was applied for the removal of organic pollutants, such as drug loperamide, from synthetic model solutions and natural river water. Waste material generated from *Lagenaria vulgaris* plants was used as a starting lignocellulosic biomass. The specific physicochemical properties of the material, reflected in its high sorption ability, are the result of combining the activity of the functional groups present in the structure of the lignocellulosic material with the applied oxide modification. In order to define the optimal conditions for the removal of loperamide from water with the lignocellulosic-Al_2O_3 hybrid, the effects of initial pH, temperature, sorbent dosage, initial loperamide concentration and hydrodynamic conditions were studied. The highest removal efficiency of loperamide was observed at neutral pH (pH from 5.0 to 8.0) and reached 99.5%, which is the greatest advantage of this hybrid, because there is no need to adjust the pH of

natural waters and typical wastewaters. The results showed that an increase in the solution temperature from 10.0 to 50.0 °C led to an increase in the removal efficiency of loperamide, indicating that the process was endothermic in nature. The extent loperamide removal is directly related to the concentration of LC-Al_2O_3 in the suspension, at an optimal biosorbent dose of 2.0 g dm^{-3}. With an increase in initial loperamide concentration, the removal efficiency decreased. Ultrasound was used as a means for enhancing the sorption process. The presence of ultrasound does not change the removal efficiency of loperamide, but it speeds up the sorption process a lot. In the absence of ultrasound, equilibrium is attained after 120 min, but in the presence of ultrasound, at power levels of 25 and 50 W, the equilibrium is attained considerably faster, after 40 and 20 min, respectively. The sorption process followed the pseudo-second order kinetics. The process can be also well described by the three-stage intraparticle and Chrastil's diffusion models, indicating that both reaction and diffusion phenomena influence the biosorption of loperamide onto the LC-Al_2O_3 hybrid. The Langmuir model and all the three-parameter isotherm models tested showed the best fit for the equilibrium of the sorption process. The calculated thermodynamic parameters showed that the biosorption of loperamide on the LC-Al_2O_3 hybrid was feasible, spontaneous and endothermic in the temperature range of 10.0-50.0 °C. The maximum sorption capacity was of 48.74 mg loperamide per g of LC-Al_2O_3 hybrid. The removal of loperamide from contaminated river water was very effective and the removal efficiency was similar to those achieved in synthetic model solutions (99.5%). In addition to the high removal efficiency, the LC-Al_2O_3 hybrid possesses other benefits, such as mechanical stability, ease of synthesis, cost-effectiveness, biocompatibility and environmental friendliness, which all make it a promising material for the removal of organic pollutants from water.

ACKNOWLEDGEMENTS: This work was financed by the Serbian Ministry of Education, Science and Technological Development through Grant No TR34008.

REFERENCES

[1] A. J. Do Ebele, M. Abou-Elwafa Abdallah and S. Harrad, *Emerging Contaminants*, **3**, 1 (2017).
[2] S. C. Monteiro and A. B. A. Boxall, *Environ. Toxicol. Chem.*, **28**, 2546 (2009).
[3] T. A. Ternes, M. Meisenheimer, D. McDowell, F. Sacher, H.-J. Brauch *et al*., *Environ. Sci. Technol*., **36**, 3855 (2002).
[4] S. R. Amirnia and M. B. Margaritis, *Chem. Eng. J*., **287**, 755 (2016).
[5] J. Huang, D. Liu, J. Lu, H. Wang, X. Wei *et al*., *Colloid. Surf. A*, **492**, 242 (2016).
[6] F. Deniz, *Desalin. Water Treat*., **51**, 4573 (2013).
[7] V. da Silva, J. B. Lopez-Sotelo, A. Correa-Guimaraes, S. Hernandez-Navarro, M. Sanchez-Bascones *et al*., *Cellulose Chem. Technol*., **51**, 127 (2017).
[8] R. P. Prajapati, M. Kalariya, S. K. Parmar and N. R. Sheth, *J. Ayurveda Integr. Med*., **1**, 266 (2010).
[9] S. M. M. Karim and P. G. Adaikan, *Prostaglandins*, **13**, 321 (1977).
[10] F. Faridbod, F. Mizani, M. Ganjali and P. Norouzi, *Int. J. Electrochem. Sci*., **7**, 7643 (2012).
[11] D. E. Baker, *Rev. Gastroenterol. Disord*., **7**, 11 (2007).
[12] G. Bertaccini, "Handbook of Experimental Pharmacology", Springer, Berlin, 1982.
[13] Y. Yang, Y. Chun, G. Sheng and M. Huang, *Langmuir*, **20**, 6736 (2004).
[14] I. Savic, G. Nikolic, I. Savic and V. Marinkovic, *Chem. Ind*., **63**, 39 (2009).
[15] H. Chaudhuri, S. Dash, S. Ghorai, S. Pal and A. Sarkar, *J. Environ. Chem. Eng*., **4**, 157 (2016).
[16] P. Roonasi and A. Y. Nezhad, *Mater. Chem. Phys*., **172**, 143 (2016).
[17] L. Wang, J. Li, Y. Wang, L. Zhao and Q. Jiang, *Chem. Eng. J*., **181**, 72 (2012).
[18] F. Wang, H. Sun, X. Ren and K. Zhang, *Chem. Eng. J*., **326**, 281 (2017).
[19] D. Yue, Y. Jing, J. Ma, C. Xia, X. Yin *et al*., *Desalination*, **267**, 9 (2011).
[20] K. J. Laidler, J. H. Meiser and B. C. Sanctuary, "Physical Chemistry", Houghton Mifflin Company, Boston, USA, 2003.
[21] T. A. Saleh, *Appl. Surf. Sci*., **257**, 7746 (2011).
[22] S. Senthilkumaar, P. Kalaamani and C. Subburaam, *J. Hazard. Mater*., **136**, 800 (2006).
[23] J. Beltrán-Heredia, J. Sánchez-Martín and M. Barrado-Moreno, *Chem. Eng. J*., **180**, 128 (2012).
[24] S. K. Bozbas and Y. Boz, *Process. Saf. Environ. Prot*., **103**, 144 (2016).
[25] B. Tural, E. Ertaş, B. Enez, S. A. Fincan and S. Tural, *J. Environ. Chem. Eng*., **5**, 4795 (2017).
[26] F. Kallel, F. Bouaziz, F. Chaari, L. Belghith, R. Ghorbel *et al*., *Process. Saf. Environ. Prot*., **102**, 30 (2016).
[27] Y. Liu, T. Liao, Z. He, T. Li, H. Wang *et al*., *Trans. Nonferrous Met. Soc. China*, **23**, 1804 (2013).
[28] M. Entezari and A. Keshavarzi, *Ultrason. Sonochem*., **8**, 213 (2001).
[29] M. H. Entezari and T. Soltani, *J. Hazard. Mater*., **160**, 88 (2008).
[30] S. K. Lagergren, *Sven. Vetenskapsakad. Handl*., **24**, 1 (1898).

[31] Y. S. Ho and G. McKay, *Process Saf. Environ.*, **76**, 183 (1998).
[32] H. Lee, E. Shim, H.-S. Yun, Y.-T. Park, D. Kim *et al.*, *Environ. Sci. Pollut. Res.*, **23**, 1025 (2016).
[33] A. Pal, S. Pan and S. Saha, *Chem. Eng. J.*, **217**, 426 (2013).
[34] W. J. Weber Jr. and J. C. Morris, *J. Sanit. Eng. Div.*, **89**, 31 (1964).
[35] D.-L. Mitic-Stojanovic, D. Bojic, J. Mitrovic, T. Andjelkovic, M. Radovic *et al.*, *Chem. Ind. Chem. Eng. Q.*, **18**, 563 (2012).
[36] W. H. Cheung, Y. S. Szeto and G. McKay, *Bioresour. Technol.*, **98**, 2897 (2007).
[37] S. J. Allen, G. McKay and K. Y. H. Khader, *Environ. Pollut.*, **56**, 39 (1989).
[38] J. Chrastil, *Text. Res. J.*, **60**, 413 (1990).
[39] F. Carrillo, M. J. Lis, X. Colom, M. Lopez-Mesas and J. Valldeperas, *Process Biochem.*, **40**, 3360 (2005).
[40] I. Langmuir, *J. Am. Chem. Soc.*, **40**, 1361 (1918).
[41] Y. S. Ho and G. McKay, *Water Res.*, **34**, 735 (2000).
[42] J. G. Flores-Garnica, L. Morales-Barrera, G. Pineda-Camacho and E. Cristiani-Urbina, *Bioresour. Technol.*, **136**, 635 (2013).
[43] H. Z. Freundlich, *J. Phys. Chem.*, **57A**, 385 (1906).
[44] A. A. Ismaiel, M. K. Aroua and R. Yusoff, *Chem. Eng. J.*, **225**, 306 (2013).
[45] H. K. Boparai, M. Joseph and D. M. O'Caroll, *J. Hazard. Mater.*, **186**, 458 (2011).
[46] G. Vázquez, M. Sonia Freire, J. González-Álvarez and G. Antorrena, *Desalination*, **249**, 855 (2009).
[47] N. Asasian, T. Kaghazchi and M. Soleimani, *J. Ind. Eng. Chem.*, **18**, 283 (2012).
[48] M. I. Temkin and V. Pyzhev, *Acta Physicochim.*, **12**, 217 (1940).
[49] O. J. Redlich and D. L. Peterson, *J. Phys. Chem.*, **63**, 1024 (1959).
[50] R. Sips, *J. Chem. Phys.*, **16**, 490 (1948).
[51] J. Toth, *Acta Chem. Acad. Hung.*, **69**, 311 (1971).
[52] A. R. Khan, I. R. Al-Waheab and A. Al-Haddad, *Environ. Technol.*, **17**, 13 (1996).
[53] A. V. Hill, *J. Physiol. (London)*, **40**, 4 (1910).
[54] F. Brouers, O. Sotolongo, F. Marquez and J. P. Pirard, *Physica A*, **349**, 271 (2005).
[55] M. C. Ncibi, S. Altenor, M. Seffen, F. Brouers and S. Gaspard, *Chem. Eng. J.*, **145**, 196 (2008).
[56] K. Vijayaraghavan, K. Palanivelu and M. Velan, *Process Biochem.*, **41**, 853 (2006).
[57] S. C. R. Santos and R. A. R. Boaventura, *J. Environ. Chem. Eng.*, **4**, 1473 (2016).
[58] M. Brdar, M. Sciban and A. Takaci, *Acta Period. Technol.*, **42**, 167 (2011).
[59] M. A. Mahmoud and M. M. El-Halwany, *J. Chromatogr. Sep. Tech.*, **4**, 1 (2013).
[60] S. M. Al-Rashed and A. A. Al-Gaid, *J. Saudi Chem. Soc.*, **16**, 209 (2012).
[61] A. U. Isah, G. Abdulraheem, S. Bala, S. Muhammad and M. Abdullahi, *Int. Biodeter. Biodegrad.*, **102**, 265 (2015).
[62] M. A. Ahsan, M. T. Islam, C. Hernandez, E. Castro, S. K. Katla *et al.*, *J. Environ. Chem. Eng.*, **6**, 4329 (2018).
[63] S. Wan, Z. Hua, L. Sun, X. Bai and L. Liang, *Process Saf. Environ. Prot.*, **104**, 422 (2016).
[64] H. Mihciokur and M. Oguz, *Environ. Toxicol. Pharmacol.*, **46**, 174 (2016).
[65] Z. Liu, X. Zhou, X. Chen, C. Dai, J. Zhang *et al.*, *J. Environ. Sci.*, **25**, 2384 (2013).
[66] S. Mondal, K. Aikat and G. Halder, *Ecol. Eng.*, **92**, 158 (2016).
[67] S. Mondal, K. Bobde, K. Aikat and G. Halder, *J. Environ. Manag.*, **182**, 581 (2016).
[68] M. Habibzadeh, N. Chaibakhsh and A. S. Naeemi, *Ecol. Eng.*, **111**, 85 (2018).
[69] R. D. S. Bezerra, M. M. F. Silva, A. I. S. Morais, M. R. M. C. Santos, C. Airoldi *et al.*, *J. Environ. Chem. Eng.*, **2**, 605 (2014).
[70] V. R. A. Ferreira, C. L. Amorim, S. M. Cravo, M. E. Tiritan, P. M. L. Castro *et al.*, *Int. Biodeter. Biodegrad.*, **110**, 53 (2016).